JOURNAL OF APPLIED ELECTROCHEMISTRY **20** (1990) 1015–1020

Electrolytic oxygen evolution on Ni–Co–P alloys

J. KUPKA, A. BUDNIOK

Institute of Physics and Chemistry of Metals, Silesian University Bankowa 12, 40-007 Katowice, Poland

Received 7 April 1989; revised 7 July 1989

Electrolytically obtained Ni–Co–P alloys exhibit amorphous structure. On heating these alloys to 773 K crystalline nickel and cobalt phosphide phases, and also nickel crystallites, are formed. After cathode–anode polarization of the amorphous and crystalline Ni–Co–P alloys in 5 M KOH for 18 h, oxygen–cobalt compounds together with crystalline or amorphous nickel phosphides appear on the electrode surface. The evolution of oxygen from 5 M KOH was studied on Ni–Co–P alloys prepared in this way. The Tafel parameters were determined and it was ascertained that the values of directional coefficients of the Tafel lines are comparable with those obtained for spinel $NiCo_2O_4$ oxides, while calculated values of the exchange currents for the oxygen evolution reaction are dependent on the chemical composition of the alloy. The rate of electrolytic oxygen evolution is virtually identical for amorphous and crystalline Ni–Co–P alloys of the same chemical composition. The highest rate of oxygen evolution was found for the alloy containing 15–20% Ni, 66–73% Co and 12–14% P.

1. Introduction

The electrode substrate material often exerts a strong influence on the course of an electrochemical process. This is associated with electrocatalytic effects, the magnitude of which depend on the type and structure of the material forming the electrode substrate. The structural parameters influencing the electrode process may be divided into (a) parameters dependent on the type of electrode substrate material, (b) those dependent on the conditions of electrode surface preparation and (c) those dependent on the electron structure of the electrode material. The type of material forming the electrode substrate, its chemical and phase composition, and also the crystallographic orientation of the substrate surface all influence the course of the electrochemical process. This is particularly clearly observable during processes taking place on the surfaces of single crystal electrodes. Structural parameters such as size of crystallites, type and number of defects, surface morphology, phase composition and texture depend on the conditions of the electrode substrate preparation. This is of special significance in the situation where the electrode surface is covered with a layer of electrolytically deposited metal. Thus it is experimentally feasible to model the electrode surface structure in such a way as to ensure its optimum influence on the magnitude of the electrocatalytic effect taking place.

Due to the fact that during the electrochemical process the electric charge passes through the phase boundary, the electron structure of the electrode substrate metal also exerts an influence on the electrochemical process. Every change in the chemical composition of the substrate brought about by the introduction of a metal or metalloid causes a change in density of the electric charge and also in the spatial siting of the molecular orbitals formed. It is then clear that the presence of new phases of the metal–metal or metal–metalloid type causes changes in the electron structure of the material in comparison with the electron structure of monometallic electrodes and, hence, also offers opportunities for the directional control of the course of the electrochemical reaction. The influence of the type and structure of the electrode substrate material, and also the influence of phases of the metal–metalloid type on the electrochemical process of oxygen evolution is explained by the occurrence of electrocatalytic effects [1–3].

It was shown that for oxide electrodes in an alkaline environment, an $NiCo_2O_4$ spinel-type phase takes part in the oxygen evolution reaction. The preparation procedure for electrodes of this type is laborious and demands precise observance of the thermal decomposition parameters of the appropriate salts and also the use of a suitable quantity of contact material. For this reason such Ni–Co metallurgical alloys were used as electrode materials for electrolytic evolution of oxygen in alkaline solutions [4]. It was also shown that on the alloy electrode surface spinel-type $NiCo_2O_4$ oxides are formed which catalyse the oxygen evolution process. As a criterion for assessing the activity of the electrode material the value of the directional coefficient of the Tafel line was taken. This value was found to lie in the interval 40–60 mV [4].

Up to now investigations have not been conducted to evaluate the suitability of electrolytic Ni–Co–P alloys as electrode materials for the electrolytic evolution of oxygen in an alkaline environment. In our earlier studies we indicated the possibility of utilizing amorphous Ni–Co–P alloys as anodes in oxygen evolution [5]. It was ascertained that the electrolytically obtained amorphous Ni–Co–P alloys, after prolonged cathode–anode cycling in 5 M KOH are suitable

0021-891X/90 $03.00 + .12

as electrode materials for oxygen evolution from an alkaline environment. Phases of type CoO(OH) and β-$Co(OH)_2$ occurring in the products of alloy oxidation and also the amorphous products of possible Ni–P oxidation, exert a catalytic influence on the evolution of oxygen. In this situation the values of the Tafel line directional coefficients are comparable with the values obtained for $NiCo_2O_4$ spinel oxides. It has not yet been elucidated, however, whether the electrocatalytic effect in the oxygen evolution process is linked only with the crystalline $CoO(OH)_2$ and β-$Co(OH)_2$ phases, or only with the products of possible Ni–P oxidation, or again with the mutual synergic reaction due to the presence of all the alloy constituents.

Recently it has been suggested that the redox system Co(II)–Co(III) exerts an electrocatalytic effect on oxygen evolution from alkaline solution [6].

The object of the investigations reported here was to examine the characteristic electrochemical behaviour of amorphous and crystalline Ni–Co–P, Ni–P and Co–P alloys in an alkaline environment and from this to ascertain the influence of alloy phase composition on the rate of electrolytic evolution of oxygen.

2. Experimental details

The Ni–Co–P alloys were obtained electrolytically from an electrolyte of composition given previously [5]. The process was conducted under galvanostatic conditions over a range of current densities from $i = 0.01$–$0.20\,A\,cm^{-2}$.

Electrodeposition took place on nickel sheet of dimensions $1 \times 1\,cm^2$. The thickness of the deposited layer was estimated by weighing and found to be about $40\,\mu m$. Prior to depositing the electrolytic layers, the nickel substrate was mechanically polished with abrasive paper and also with diamond paste. The substrate was then washed with distilled water, degreased, dried and weighed, immersed for 3–5 s in a 1 : 3 solution of HNO_3 and then, after rewashing, it was used for alloy deposition. The thickness of alloy deposited was determined by weighing.

The Ni–P and Co–P alloys were obtained from electrolyte solutions of the same composition as for Ni–Co–P alloy electrodeposition, minus the appropriate cobalt or nickel salts.

Chemical analysis of the alloy layers obtained was by atomic absorption spectrophotometry. Alloy layers for chemical analysis were deposited on a copper substrate. After being dissolved in HNO_3 (1 : 1) followed by suitable dilutions, the cobalt, nickel and phosphorus contents were determined. Results obtained were compared with the alloy mass determined by the weighing method. The error in estimation of the sum of masses of the elements was 5%.

Immediately after electrodeposition of all the alloys, structural examinations were made by the X-ray diffraction method, using a Philips diffractometer and $Cu_{K\alpha}$ radiation. Some of the samples were then thermally treated in a furnace in an argon (99.99%) atmosphere at 773 K for 1 h, after which the structure of the electrolytic layers was determined. Proceedings in this way for each chemical composition of the alloy five amorphous layers and five crystalline layers of alloy were obtained.

The layers of electrolytic alloy prepared in this way were next electrochemically treated in 5 M KOH. Alloy electrodes were placed in a standard electrochemical vessel. Electrode potential was measured relative to a saturated calomel electrode (SCE) via a Haber–Luggin capillary. The KOH solution was of analar purity (Merck) and double distilled water was used. Tests were carried out at a temperature of 298 K.

The alloy electrodes were subjected to cyclic linear cathode–anode polarization in the range from the potential of hydrogen evolution to the potential of oxygen evolution. Cycling was commenced from the rest potential of the electrode in the solution in the anode direction. Cycling was maintained for 18 h. The rate of change of electrode potential was $20\,mV\,s^{-1}$. Tests were conducted using an EP-20 potentiostat and an EG-20 generator. The i–E relations were recorded using an Endim recorder.

After completing the electromechanical treatment the alloy electrodes were again subjected to structural tests in order to determine the phase composition of the products of anode oxidation of the amorphous and crystalline electrolytic alloys.

The characteristic parameters of the process of oxygen evolution on amorphous and crystalline alloys were determined using the potentiodynamic method with the aim of calculating the Tafel parameters. For this purpose each electrode was polarized at a potential of $E = 0.650\,V$ for 10 min, during which time a large quantity of oxygen was given off. Then during the linear depolarization of the electrodes at a rate of $v = 1\,mV\,s^{-1}$ the relation i–E was recorded up to a potential of $E = 0.500\,V$. From the curves obtained, and after converting the potential relative to a hydrogen electrode, the Tafel curves were plotted for the various types of alloys. Values of exchange current density were calculated and the rates of oxygen evolution on the various alloys were compared.

3. Discussion of results and conclusions

The chemical composition of the electrolytic alloys depends on the conditions in which they were obtained. It was found that with an increase in current density the nickel content in the Ni–Co–P alloy coatings also increased from 2.7% to 46%, while the phosphorus content decreased from 16.6% to 11%. With an increase in the current density of the electrolytic process for obtaining Ni–Co–P alloy, the cobalt content also decreased from 80.7% to 43% (Table 1).

X-ray examination of the nickel and cobalt with phosphorus alloys and also the Ni–P and Co–P alloys indicated that they all exhibited amorphous structure. This is shown by the occurrence of broad peaks on the diffraction patterns obtained for all the tested alloys

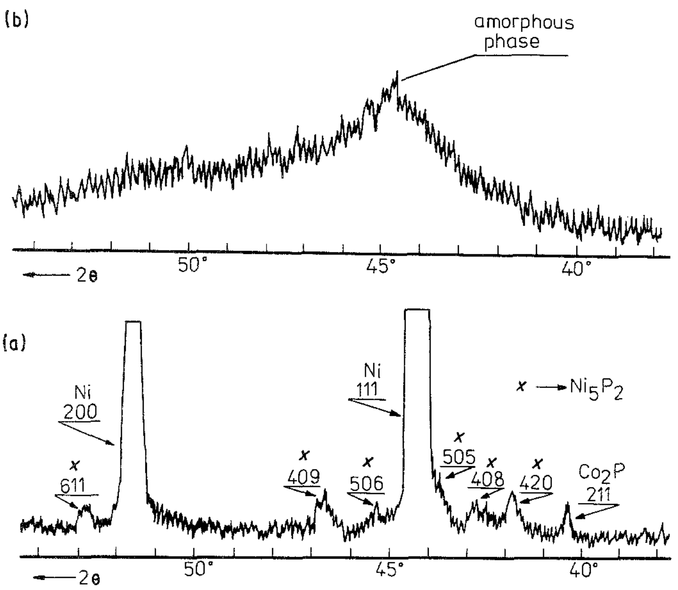

Fig. 1. Diffraction pattern for Ni–Co–P alloy obtained at current density $j = 0.20\,\mathrm{A\,cm^{-2}}$ for (a) alloy annealed for 1 h at 773 K and (b) alloy after electrolytic deposition.

(Fig. 1). The occurrence of this amorphous state is associated with the presence of phosphorus.

Heating the electrolytic alloys at 773 K causes a change in structure due to the crystallization of phases from the amorphous system. This effect is very distinctly visible on the diffraction patterns in the form of sharp well-formed peaks characteristic of crystalline substances (see Fig. 1). In electrolytic Ni–P alloys the presence of nickel phosphides (Ni_5P_2) and nickel crystallites was detected. As a consequence of isothermal crystallization the Co–P alloys pass entirely to the Co_2P phase. In electrolytic Ni–Co–P alloys subjected to heating, the presence of nickel and cobalt crystallites was ascertained and also the presence of nickel and cobalt phosphides. The relative intensity of the diffraction lines of the particular phases is dependent on the chemical composition of the Ni–Co–P alloy.

Prolonged cyclic cathode–anode polarization of amorphous and crystalline nickel and cobalt alloys with phosphorus causes a change in their phase composition. This fact was established from analysis of the X-ray diffraction patterns of the products of cyclic cathode–anode polarization of alloys. In amorphous Ni–Co–P alloys, independent of the chemical composition, the presence of CoO(OH), β-$Co(OH)_2$ and α-Co phases was detected. Reflection from the spinel $NiCo_2O_4$ phase was not detected. Also no other crystalline phase reflection was found. Nevertheless, from higher values of the background it may be taken that the electrochemical treatment applied did not cause the destruction of the amorphous nickel chemical compounds. Corroboration of this conclusion was found in structural studies conducted after prior prolonged cyclic cathode–anode polarization of the amorphous Ni–P alloy.

Table 1. Chemical composition of Ni–Co–P alloys (% weight), conditions in which they are obtained (j) and also Tafel equation parameters for the process of electrolytic oxygen evolution.

Lp	*j A/cm²*	*%Ni*	*%Co*	*%P*	*Tafel equation for amorphous (A) and crystalline (K) alloys*	j_0 *A/cm²*
1	0.01	2.7	80.7	16.6	A: $\eta = 0.320 + 0.045\,\lg j$ K: $\eta = 0.337 + 0.047\,\lg j$	$7.72 \cdot 10^{-8}$ $6.53 \cdot 10^{-8}$
2	0.10	15.1	71.2	13.7	A: $\eta = 0.344 + 0.051\,\lg j$ K: $\eta = 0.351 + 0.053\,\lg j$	$1.79 \cdot 10^{-7}$ $2.32 \cdot 10^{-7}$
3	0.15	19.0	69.0	12.0	A: $\eta = 0.346 + 0.053\,\lg j$ K: $\eta = 0.362 + 0.055\,\lg j$	$2.95 \cdot 10^{-7}$ $2.55 \cdot 10^{-7}$
4	0.20	46.0	43.0	11.0	A: $\eta = 0.290 + 0.040\,\lg j$ K: $\eta = 0.324 + 0.045\,\lg j$	$5.61 \cdot 10^{-8}$ $6.25 \cdot 10^{-8}$
5	0.10	88.5	–	11.5	A: $\eta = 0.464 + 0.063\,\lg j$ K: $\eta = 0.430 + 0.058\,\lg j$	$4.30 \cdot 10^{-8}$ $3.73 \cdot 10^{-8}$
6	0.10	–	87.5	12.5	A: $\eta = 0.456 + 0.054\,\lg j$ K: $\eta = 0.436 + 0.052\,\lg j$	$3.58 \cdot 10^{-9}$ $4.12 \cdot 10^{-9}$

Following electrochemical treatment this alloy maintained its amorphous structure. It may be postulated that, after oxidation of the amorphous Ni–P alloys in an alkaline environment, amorphous products of this oxidation are obtained: or again, that their quantity in the crystalline form is too small to be observed in X-ray studies. Electrochemical treatment of amorphous Co–P alloy leads to the formation of the same cobalt crystalline phases as those which formed in the Ni–Co–P system.

In the Ni–Co–P crystalline alloys, independent of the chemical composition, after prolonged cyclic cathode–anode polarization, the presence of α-Co, Ni, CoO(OH), β-$Co(OH)_2$ and Ni_5P_2 crystallites was detected. The presence of Co_2P phase diffraction lines initially occurring in the alloy was not ascertained. There was also no confirmation of the occurrence of spinel $NiCo_2O_4$ phases catalysing the oxygen evolution process in an alkaline environment, nor of crystalline phases from the products of nickel oxidation. The presence of Ni_5P_2 in the surface layer indicates its very high resistance to cyclic polarization in an alkaline environment.

Change of the chemical composition of the Ni–Co–P alloys and also of the thermal treatment applied had no significant effect on the mode of change of the

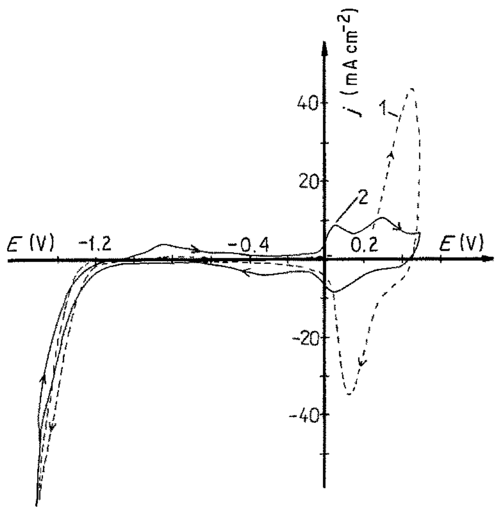

Fig. 2. Function i–E in a 5 M KOH solution for Ni–Co–P amorphous alloys containing (1) 46% Ni and (2) 19% Ni (v = 20 mV s^{-1}).

phase composition after cyclic electrode polarization in a KOH solution.

During the linear cyclic polarization of amorphous and crystalline Ni–Co–P alloy in a potassium hydroxide solution in the range from the potential of hydrogen evolution to the potential of oxygen evolution, oxidation peaks were found to occur on the chronovoltamperometric curve. The number and position of these peaks relative to the potential axis, and also the height of these peaks, are dependent on the chemical composition of the alloy and on polarization time (Figs 2 and 3).

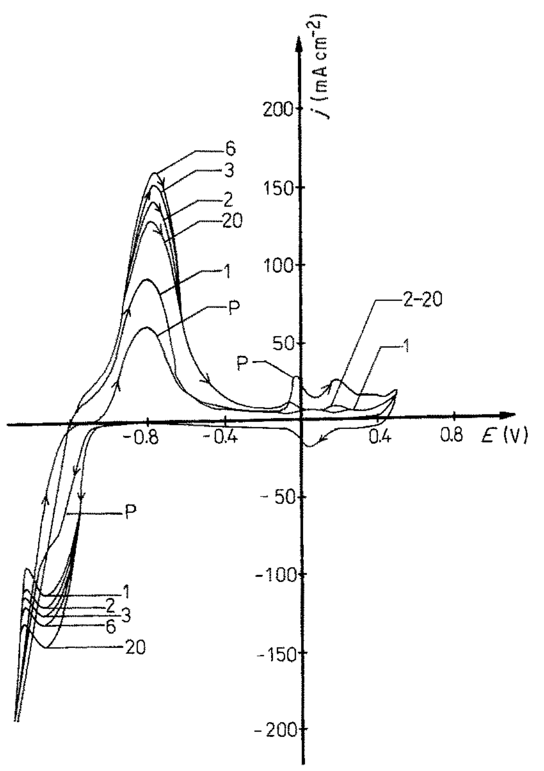

Fig. 3. Functions i–E in a 5 M KOH solution found for a crystalline Ni–Co–P alloy containing 2.7% Ni (v = 20 mV s^{-1}). Lines 1–20 are successive polarization cycles; P is function i–E after 18 h polarization.

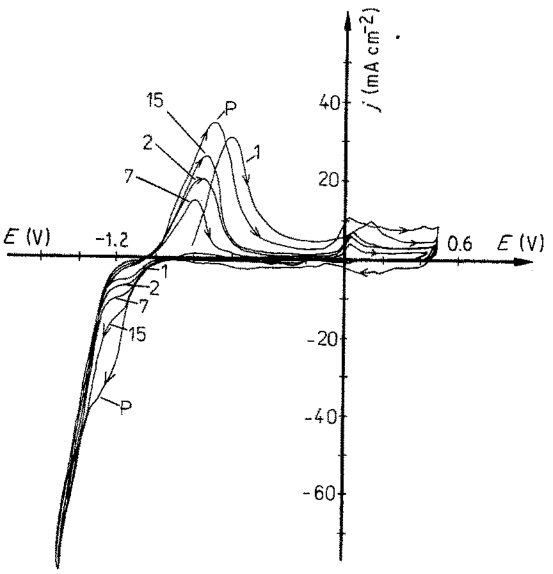

Fig. 4. Function i–E in 5 M KOH solution found for amorphous Co–P alloy (v = 20 mV s^{-1}). Lines 1–15 are successive polarization cycles; P is function i–E found after 18 h cyclic polarization.

For Ni–Co–P alloys containing up to 19% Ni, three oxidation peaks are found on the i–E curves. The presence of these peaks is associated with the electrochemical oxidation of Co_2P, $Co(OH)_2$ and nickel, irrespective of whether the alloy is amorphous or crystalline. The first oxide peak, occurring at negative potentials, is associated with the electrooxidation of Co_2P. This peak has an oxidation potential value comparable with that for the peak obtained on the i–E curves for the Co–P system (Fig. 4). In this case the phosphorus is completely bound in the Co_2P, which is particularly clearly visible on the X-ray diffraction patterns after heating the amorphous alloy. Hence during anode polarization, electrooxidation takes place according to:

$$Co_2P + 3H_2O + OH^- \rightleftharpoons 2Co(OH)_2 + PH_3 + e^- \quad (1)$$

The nature of the Co_2P oxidation peak is dependent on the time of cyclic polarization (see Fig. 4). Initially the values of peak current increase and with further polarization of the electrode these peak current values

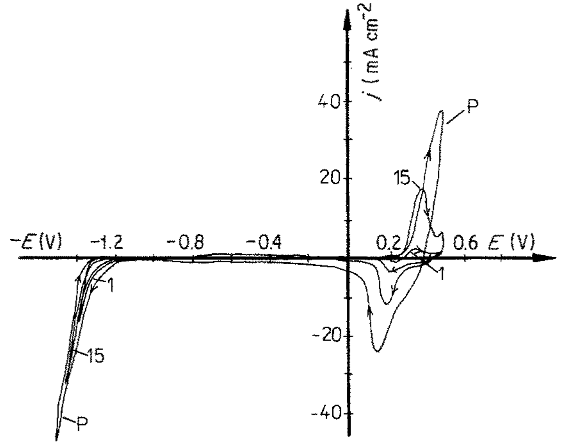

Fig. 5. Function i–E in 5 M KOH solution obtained for crystalline Ni–P alloy (v = 20 mV s^{-1}). Lines 1–15 are successive polarization cycles; P is function i–E after 18 h cyclic polarization.

decrease. This is accompanied by shifting of the peak potential towards more positive values. This type of behaviour of the peak is observed for amorphous and crystalline Ni–Co–P alloys and becomes even more distinct with a reduction in nickel content in the alloy (see Fig. 3).

In Ni–Co–P alloys containing 46% Ni no peak corresponding to the Co_2P oxidation reaction was found (see Fig. 2). It may be postulated that this is due to the small quantity of this phase and the rapid rate of its electrooxidation so that no corresponding peak is observed on the *i–E* curve. The alloy of this type behaves similarly to the Ni–P alloy containing only Ni and Ni_5P_2. On the *i–E* curve obtained for the Ni–P alloy no peak corresponding to the oxidation of nickel phosphides was found, and at positive potentials only one oxidation peak occurred (Fig. 5).

The second and third peaks on the anode segment of the *i–E* curve obtained for the Ni–Co–P alloy containing up to 19% Ni are associated with the reaction of oxidation of compounds Co(II) to Co(III), and with the oxidation of nickel (II) oxides due to the passivation of nickel in the alkaline environment:

$$Co(OH)_2 + OH^- \rightleftharpoons CoO(OH) + H_2O + e^- \qquad (2)$$

$$Ni(OH)_2 + OH^- \rightleftharpoons NiO(OH) + H_2O + e^- \qquad (3)$$

These oxidation reactions may be observed separately on the *i–E* curves obtained for Co–P and Ni–P alloys, irrespective of the treatment applied (see Figs 4 and 5).

On the chronovoltamperometric curves obtained for Ni–Co–P alloys containing 46% Ni no separate oxidation peak associated with Reaction 2 was found. Since, however, analysis of the phase composition shows the presence of CoO(OH) it may be assumed that due to the passivation action of nickel phosphides, in the Ni–Co–P alloys the potential of oxidation according to Reaction 2 shifts towards more positive values and coincides with the potential of formation of NiO(OH).

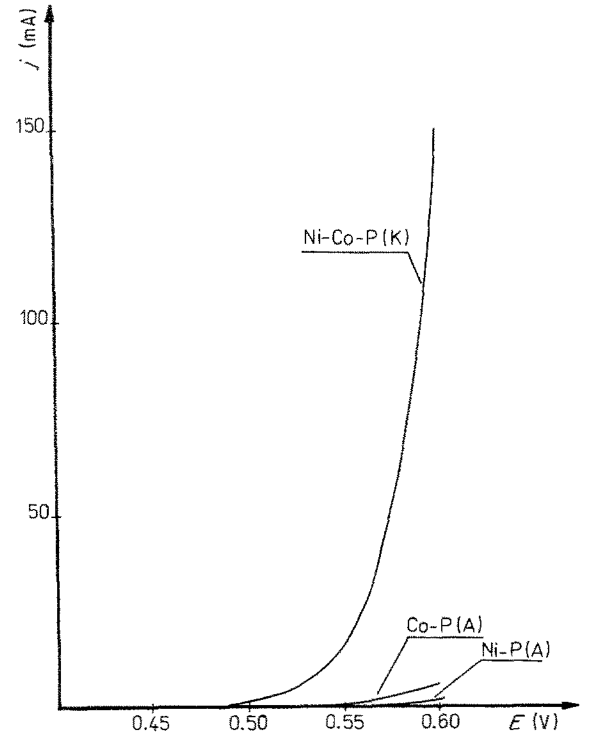

Fig. 6. Potentiodynamic curves obtained from 5 M KOH solution for (K) crystaline alloys and (A) amorphous alloys (T = 298 K, v = 1 mV s^{-1}).

During cathode–anode polarization the surface of the Ni–Co–P alloys underwent alternating oxidation and reduction processes. The irreversibility of the Co_2P reduction and oxidation causes a gradual covering of the surface with the products of its oxidation and an increase in the electrochemically active electrode surface. This occurrence is governed by the relation between the current at particular oxidation and reduction peaks and the time of cyclic polarization. After prolonged (18 h) electrode polarization the form of the *i–E* curve becomes independent of time and equilibrium exists between the products formed. Electrodes prepared in this way were used to compare the characteristic parameters of the oxygen evolution process. For this purpose the parameters of the Tafel equation were determined from the potentiodynamic curves obtained for each amorphous and crystalline alloy system (Fig. 6). Taking into consideration the equilibrium potential of the oxygen electrode in the alkaline environment (E = 0.401 V) [7] and also the value of the potential of the SCE, the Tafel parameters were estimated. The coefficient of linear correlation lay in the range 0.991–0.999.

From the Tafel lines it was possible to ascertain that the directional coefficients, irrespective of the heat treatment applied, lie in the interval from 0.040–0.063 and are comparable with the values obtained for the oxygen evolution process on $NiCo_2O_4$ [4].

The calculated values of exchange current density, j_0, characterising the ability for electrolytic oxygen evolution on particular types of alloys, shows a rising trend with a rise in nickel content in the alloys to 19%. This trend is observable both in crystalline and amorphous alloys. A further rise in nickel content in the Ni–Co–P alloys to 46% causes a reduction in the value of exchange current density, j_0 (Fig. 7). Irrespective of the heat treatment applied, both in the Ni–P and Co–P alloys the values of exchange current density are distinctly less than those obtained for Ni–Co–P alloys. In the Ni–Co–P alloy, at small values of Ni the value of exchange current density is already higher than for Ni–P and Co–P alloys. From this it may be concluded that the joint presence of Ni_5P_2, β-$Co(OH)_2$ and CoO(OH) phases, and very probably also the amorphous products of Ni oxidation to NiO(OH), induces the electrocatalytic effect of oxygen evolution on the electrolytic Ni–Co–P alloys in the alkaline environment. However, the influence of these phases on the value of the exchange current cannot be estimated definitively. The electrocatalytic effect is thus more dependent on the chemical composition of the alloy undergoing irreversible oxidation in the cyclic polarization process.

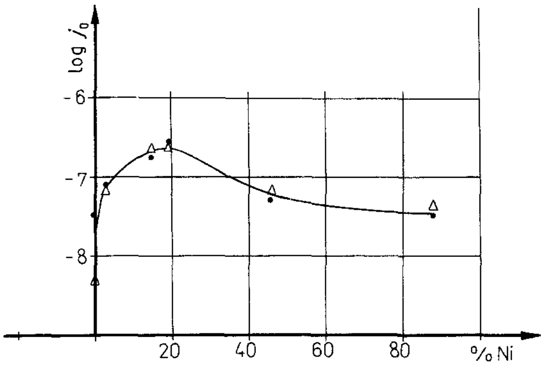

Fig. 7. Function of $\log j_0$ against percentage nickel content in Ni–Co–P alloys.

This effect may be explained by the synergetic influence of the joint presence, in specific proportions, of all the phases obtained by suitable electrochemical treatment of an electrolytic alloy containing 15–20% Ni, 12–14% P and 66–73% Co. Most probably these phases act together in the process of electrolytic oxygen evolution according to the mechanism:

$$\mathrm{CoO(OH)} + 3\mathrm{OH^-} \rightleftharpoons \mathrm{Co(OH)_2} + \mathrm{H_2O} + \mathrm{O_2} + 3e^- \quad (4)$$

$$\mathrm{Co(OH)_2} + \mathrm{OH^-} \rightleftharpoons \mathrm{CoO(OH)} + \mathrm{H_2O} + e^- \quad (5)$$

or in summary form:

$$4\mathrm{OH^-} \rightleftharpoons 2\mathrm{H_2O} + \mathrm{O_2} + 4e^- \quad (6)$$

The possibility of amorphous products, e.g. NiO(OH) or $\mathrm{Ni(OH)_2}$ participating in a similar electrode reaction mechanism cannot be excluded. Hence the evolution of oxygen on such alloys may be associated with the presence of the $\mathrm{CoO(OH)} \rightleftharpoons \mathrm{Co(OH)_2}$ system which exerts an electrocatalytic effect on the oxygen evolution process. This is in agreement with the results obtained by Markina and Tarasewith [6]. The Ni–Co–P alloys were obtained at various current densities; therefore their surface morphology and degree of surface development exert a specific influence on the electrocatalytic effect.

Acknowledgement

The authors wish to express their thanks for financial assistance in support of this research in the programme CPBP 01.15.

References

[1] J. Haenen, W. Visscher and E. Barendrecht, *J. Appl. Electrochem.* **15** (1985) 29.
[2] W. J. King and A. C. C. Tseung, *Electrochim. Acta* **19** (1974) 485.
[3] J. Haenen, W. Visscher and E. Barendrecht, *J. Electroanal. Chem.* **208** (1986) 273.
[4] *Idem*, *Electrochim. Acta* **31** (1986) 1541.
[5] A. Budniok and J. Kupka, *ibid* **34** (1989) 871.
[6] E. Markina and M. Tarasewith, *Electrochimija* **24** (1988) 93.
[7] R. Parsons (ed.), 'Handbook of Electrochemical Constants', Butterworths Scientific Publications, London (1959).